

Short communication

I₂/TBHP promoted isocyanide insertion cyclization reaction for the synthesis of quinazolin fused benzoimidazole as a selective methanol detection probe

Fereshteh Ahmadi^a, Nafiseh Ahmadi^b, Yaser Balmohammadi^a,
 Mohammad Reza Naimi-Jamal^{b,*}, Ayooob Bazgir^{a,*}

^a Department of Organic Chemistry, Shahid Beheshti University, Tehran 1983963113, Iran

^b Department of Chemistry, Iran University of Science and Technology, 16846 Tehran, Iran



ARTICLE INFO

Keywords:

I₂/TBHP catalyst
 Isocyanide insertion reactions
 Benzoimidazoquinazolins
 Methanol detection
 Fluorescence probe

ABSTRACT

An efficient I₂/TBHP promoted isocyanide insertion cyclization reaction for the synthesis of quinazolines-fused benzoimidazole was reported. The synthesized compounds have a unique potential to use as a selective solvatochromic fluorescence probe for methanol detection from other solvents, especially EtOH. Introducing a simple one-step method and using a more acceptable iodine molecule instead of expensive transition metal catalysts are the most important advantages of this strategy.

1. Introduction

Cyclization reactions using an isocyanide insertion strategy are powerful methods for synthesizing various cyclic organic compounds [1–4]. Although most of these reactions are catalyzed by transition metals such as Pd, Ni, Co, Rh, Mn, and Cu [1–4], the metal coordination of isocyanides and their polymerization using transition metals lead to the reduction of catalytic activity [5]. Very recently, the metal-free I₂-catalyzed isocyanide insertion cyclization reaction is a significant challenge for chemists to synthesize the potentially active heterocycles [6–8]. Compared to transition metals, iodine is an inexpensive, readily available, environmentally friendly, and nontoxic catalyst [9].

Recently, a number of dyes have been used in the detection of toxic substances [10,11]. Methanol as a hazardous compound leads to some illnesses in optic and nervous systems and may progress to death. It has omnipresent use as raw material and solvent in various industries and research laboratories. Therefore, methanol level detection is necessary and significant in chemical and pharmaceutical industries [12,13]. The HPLC, GC, UV–visible, FTIR spectroscopy, electrochemical, and enzymatic amperometric techniques have been reported for the methanol detection. Some of these methods are tedious and need complex pretreatment and high-cost instruments [12,13]. The instability of enzyme electrodes under harsh conditions and toxic chemicals pose practical concerns in some electrochemical techniques [13]. Thus,

significant attention has been attracted to introducing new applicable, efficient, cheap, and quick techniques for the detection of methanol [14–16]. Because of simplicity, sensitivity, fast response times, and the monitoring of the trace amounts of substances, fluorescent spectroscopy is an ideal candidate to achieve the goal [17–21].

Very shortly, the synthesis of some new solvatochromic fluorescence compounds has been developed for methanol recognition without any investigations on the methanol-ethanol discrimination [22–24]. Due to same properties of methanol and ethanol, the careful discrimination of methanol over ethanol is an important and needful task. Despite its importance, the number of reports on the synthesis of solvatochromic fluorescence compounds for the efficient MeOH–EtOH distinction in solutions are rare [25–27]. Encouraged by these reports, herein, we report a facile and straightforward I₂/TBHP catalyzed cyclization reaction using isocyanide insertion for the benzoimidazoquinazolins synthesis. The synthesized scaffold can be used as a selective solvatochromic fluorescence probe for methanol detection.

2. Experimental

2.1. Materials and methods

Melting points were determined with a melting point Thermo Scientific 9100 apparatus and are uncorrected. IR spectra were taken with a

* Corresponding authors.

E-mail address: a_bazgir@sbu.ac.ir (A. Bazgir).

<https://doi.org/10.1016/j.catcom.2021.106331>

Received 24 January 2021; Received in revised form 27 April 2021; Accepted 7 June 2021

Available online 8 June 2021

1566-7367/© 2021 Published by Elsevier B.V. This is an open access article under the CC BY-NC-ND license (<http://creativecommons.org/licenses/by-nc-nd/4.0/>).

Bomem FT-IR MB spectrometer. NMR spectra were recorded with 300 MHz Bruker DRX Avance spectrometers. Mass spectra were recorded with an Agilent Technologies (HP) 5973 mass spectrometer. UV-Vis spectra were recorded on a Shimadzu 2100 spectrometer using a 1-cm path length cell at room temperature, and the fluorescence spectra were recorded on a Perkin Elmer LS 45, using a 1-cm path length cell. The X-ray diffraction measurements were made with a STOE IPDS-II diffractometer with graphite-monochromated MoKa radiation. All chemicals were purchased from Merck or Aldrich and were used without further purification. The 2-(4,5-diphenyl-1H-imidazol-2-yl)aniline **5** was synthesized according to a literature report [28].

2.2. General procedure for the synthesis of benzoimidazoquinazoline amines (**3**)

Isocyanide (0.75 mmol) was added to a stirred solution of 2-(1H-benzo[d]imidazol-2-yl)aniline (0.5 mmol), I₂ (0.1 mmol) and TBHP (70% aqueous solution, 1 mmol) in 1,4-dioxane (1 mL). The mixture was then kept under stirring at 100 °C for 12 h. After that, the concentrated residue was purified by the column chromatography over silica gel using n-hexane/ethyl acetate (4:1) as eluent to give the desired product **3**.

3. Results and discussion

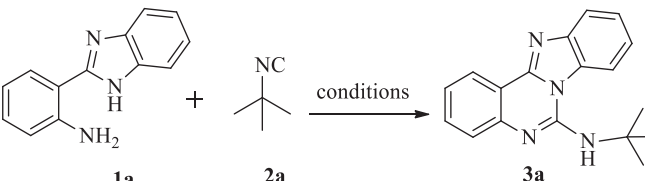
Our investigation was initiated by the reaction of benzo[d]imidazol-aniline **1a** and tert-butyl isocyanide **2a** using 20 mol% I₂ as the catalyst and TBHP as the oxidant in MeCN at 100 °C for 12 h. The benzoimidazoquinazolin-6-amine **3a** was produced in 39% yield (Table 1, entry 1). To improve the yield, various reaction conditions were then tested. First, the solvent screening (entries 1–9) revealed that

the 1,4-dioxane is the superior solvent for the reaction, and the **3a** was obtained in 63% isolated yield (entry 5). Then, the effect of iodine in the reaction was checked. In the absence of iodine, only a trace amount of **3a** was produced (entry 10). Next, the other amounts of catalyst was tested in the reaction using 10, 15 and 25 mol% of catalyst (Table 1, entries 11–13). The 20 mol% of catalyst afforded the best isolated yield (entry 5). Notably, no better result was observed by removing the oxidant (Table 1, entry 14). Subsequently, some commercially available oxidants such as BPO, K₂S₂O₈, H₂O₂ and Ag₂CO₃ were screened in the reaction (entries 15–18). As shown, the reaction worked most efficiently in the presence of TBHP as an oxidant (entry 5). We tested the reaction at room temperature and 50 °C. It was found that the **3a** was obtained in lower yields (entries 19 and 20). Finally, the other iodine sources such as NIS, KI, and CuI were tested in the reaction [29–31]. As shown in Table 1, the product **3a** was obtained in low yield (entries 21–23). Therefore, the 1,4-dioxane using 20 mol% iodine in the presence of TBHP at 100 °C was chosen as the optimized reaction conditions.

Then, the reaction of various benzimidazoloanilines with different isocyanides was carried out to investigate the generality of the method (Scheme 1). The reaction of substituted benzo[d]imidazol-2-yl anilines with aromatic and aliphatic isocyanides successfully afforded the **3a-1** in moderate to high isolated yields.

To achieve more information about the reaction mechanism, a control radical trapping experiment was conducted using TEMPO as a radical scavenger to trap possible radical intermediates. Surprisingly, no considerable change took place, and the desired product **3a** produced in 60% yields, thus indicating the no radical mechanism (Scheme 2, eq. 1). When the reaction was carried out by the *N*-methyl imidazole derivative **4** or nitro-phenyl imidazole **5** under the standard reaction condition, the TLC and ¹H NMR spectra of the reaction mixture showed a combination

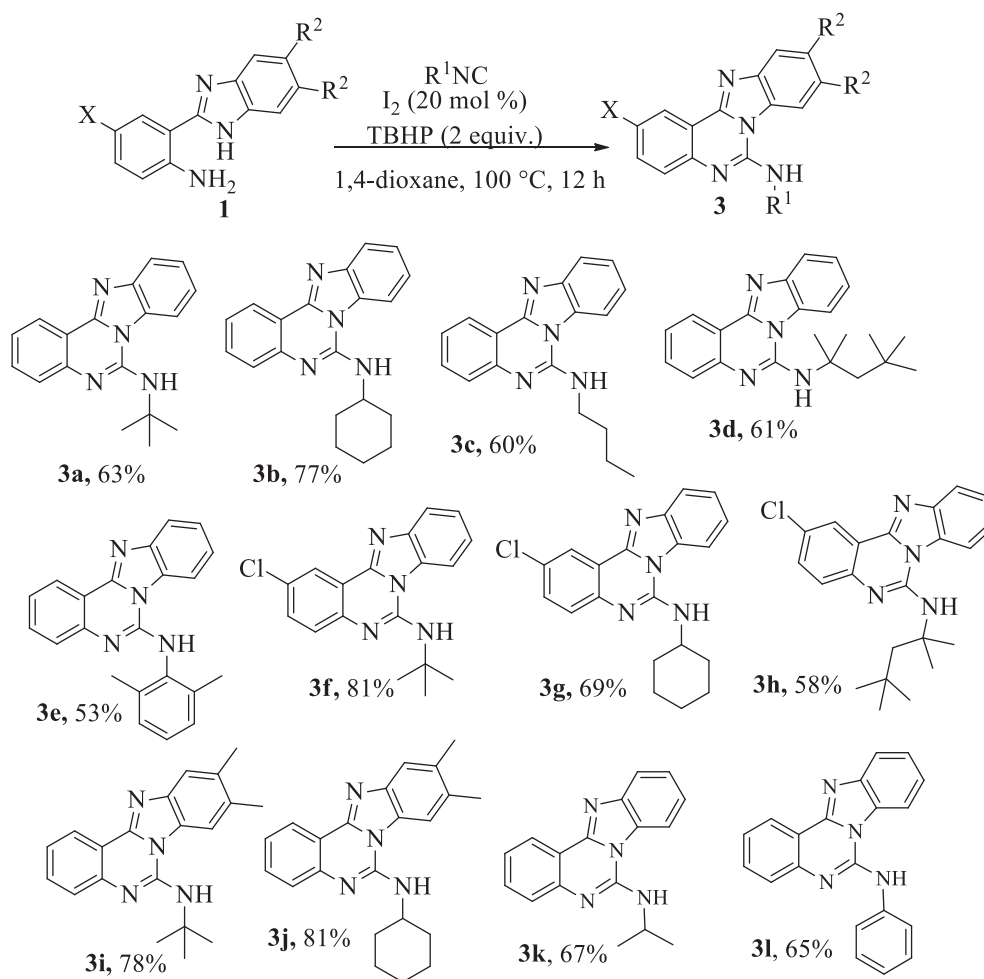
Table 1
Optimization of the reaction conditions^a.



Entry	Solvent	I ₂ (mol%)	Oxidant	Yield [%]
1	CH ₃ CN	20	TBHP	39
2	<i>t</i> BuOMe	20	TBHP	43
3	DCM	20	TBHP	35
4	PhCH ₃	20	TBHP	59
5	1,4-Dioxane	20	TBHP	63
6	H ₂ O	20	TBHP	trace
7	THF	20	TBHP	33
8	DMF	20	TBHP	19
9	DMSO	20	TBHP	25
10	1,4-Dioxane	–	TBHP	trace
11	1,4-Dioxane	10	TBHP	49
12	1,4-Dioxane	15	TBHP	54
13	1,4-Dioxane	25	TBHP	60
14	1,4-Dioxane	20	–	18
15	1,4-Dioxane	20	BPO	59
16	1,4-Dioxane	20	K ₂ S ₂ O ₈	54
17	1,4-Dioxane	20	H ₂ O ₂	48
18	1,4-Dioxane	20	Ag ₂ CO ₃	60
19 ^b	1,4-Dioxane	20	TBHP	trace
20 ^c	1,4-Dioxane	20	TBHP	27
21 ^d	1,4-Dioxane	20	TBHP	25
22 ^e	1,4-Dioxane	20	TBHP	<20
23 ^f	1,4-Dioxane	20	TBHP	28

^a 2-amino-*N*-benzylbenzamide (0.5 mmol), *t*-BuNC (0.75 mmol), I₂ (20 mol%), oxidant (2 eq), solvent (2.0 mL), 100 °C, 12 h.

^b room temperature. ^c 50 °C. ^dCat. = NIS. ^eCat. = KI. ^fCat. = CuI.



Scheme 1. Synthesis of benzoimidazoquinazoline **3**.

Isocyanide (0.75 mmol), 2-(1H-benzo[d]imidazol-2-yl)aniline (0.5 mmol), I₂ (0.1 mmol), TBHP (1 mmol), 1,4-dioxane (1 mL) at 100 °C for 12 h.

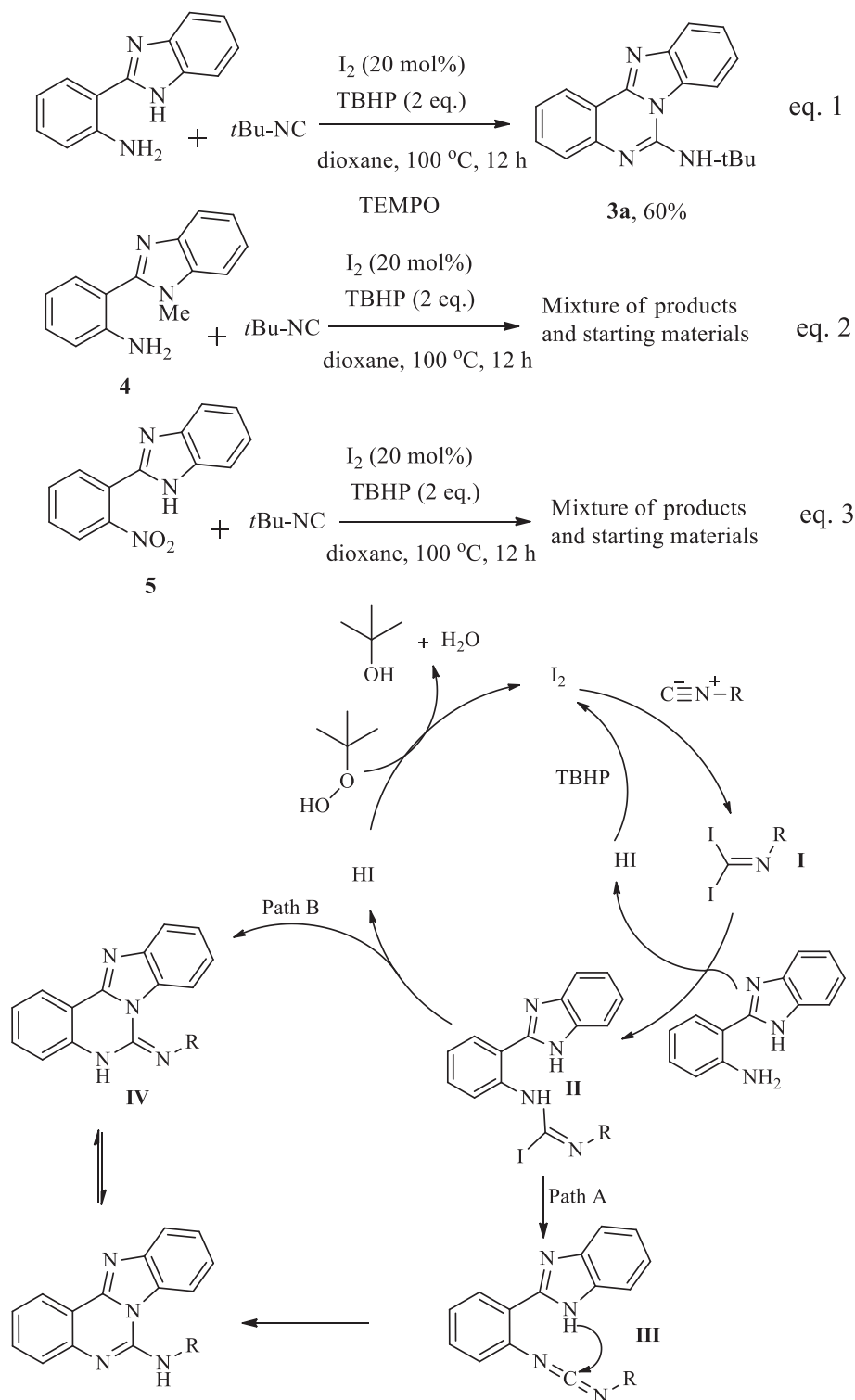
of starting materials and several products (Scheme 2, Eq. 2 and 3). Based on the current study results and referring to the previous literature reports [8], we propose a plausible mechanism for the reaction (Scheme 2). It seems the Lewis acidity of iodine shows enormous catalytic activity making it capable of binding with the isocyanide to form the desired intermediate I. Then, intermediate I reacts with benzimidazole aniline 1 to result in intermediate II and HI through dehydrohalogenation. The HI is oxidized by TBHP, giving iodine, and then completes the cycle. There are two possible pathways for the second dehydrohalogenation of intermediate II. In Path A, dehydrohalogenation leads to carbodiimide III formation, and finally, intramolecular cyclization of III affords the product. The other plausible pathway for forming the final product (Path B) involves the formation of IV by intramolecular cyclization. Then, the tautomerization of IV gives the final product.

Recently, the aminophenylbenzimidazole based structures have been reported as probes for detecting toxic substances [32,33]. Consequently, photophysical behavior of the synthesized scaffold was evaluated by absorption and emission spectroscopy. Due to different solvation of the ground and excited states for a light-absorbing molecule, the photophysical behavior of solvatochromic materials depends on media [34,35]. Therefore, the solvatochromic behavior of **3a** was investigated at room temperature in various polar solvents like DCM, dioxane, DMF, DMSO, EtOH, isopropyl alcohol (IPA), and MeOH (Fig. 1). Almost the same behavior was observed for **3a** in all solvents (Fig. 1-left). It showed a maximum absorption at about 269–274 nm in these solvents (ESI, Table S1). In aprotic solvents, the emission behavior of **3a** was almost similar, including an emission peak at 374–386 nm (Fig. 1-right,

Table S1). Probably, a little separation of charge or no significant stabilization of solvent can be considered within **3a**. Notably in MeOH, a major blue shift was observed (325 nm). The compounds **3g** and **3j** showed similar behavior (ESI). The Stokes shift of **3a** showed the highest values (9924–10,630 cm⁻¹) in aprotic polar solvents while the lowest Stokes shift value (6405 cm⁻¹) in MeOH as a protic solvent. The particular property of **3a** in MeOH could consider from the hydrogen bonding formation of **3a** with MeOH. We assumed that the formation of H-bonded coordination pairs with methanol could form new conformational isomers [13], solidifying selective discrimination through spectral changes (Scheme 3).

The DFT calculations were used to support the hydrogen bonding pair formation in MeOH. All calculations were done using DFT and time-dependent DFT (TDDFT) methods. The B3LYP and m062-x functionals with 6–31 + G(d,p) and Def2-TZVP basis sets were used in the calculations. The polarizable continuum model (PCM) and the conductor-like polarizable continuum model (CPCM) were considered the solvent effect. The molecular orbital diagrams are plotted by Gauss View 5.1 software. All calculations were done by the Gaussian 09 W software package. The compound **3a** adapted two different structures (ESI, Fig. S5). The structure optimization results of these geometries based on B3LYP and M062-X functionals along with the 6–31 + G(d,p) and Def2-TZVP basis sets demonstrated that isomer 1 with in-plane tert-butyl is more stable (–0.325 eV) and (–0.209 eV) than isomer 2 without of the plane tert-butyl group.

The ability of hydrogen bonding pair formation of **3a** with methanol can overcome this difference. According to Fig. S5, isomers 1 and 2 have



Scheme 2. The control experiments and the reaction mechanism

enough free space around the nitrogen of benzimidazole moiety (N3) to form a H-bond with MeOH. The in-plane *tert*-butyl group in isomer 1 makes steric effects for hydrogen bond formation in other sites (N2 and NH groups). In isomer 2, the out-of-plane *tert*-butyl group does not have a steric effect to disrupt the hydrogen bond formation of MeOH with N2. In addition, the oxygen atom of the methanol can form a hydrogen bond with the NH group. This behavior was examined by DFT calculations. The hydrogen-bonded structures of **3a** were optimized in B3LYP/Def2-TZVP computational level, and the thermodynamic parameters (ΔE ,

ΔH , and ΔG) were calculated (ESI, Table S2). Although isomer 1 is more stable than isomer 2 but based on Table S1, the ΔE , ΔH , and ΔG of F2-(MeOH)₂ is more negative than F1-MeOH. In other words, the interaction of isomer 2 with methanol is easier and more spontaneous than isomer 1. As a result, the hydrogen-bonded coordination pair formation in MeOH makes conformational isomer 2.

The ability of hydrogen bonding pair formation of **3a** with EtOH has been provided in ESI. A similar trend was observed for EtOH. However, the thermodynamic parameters for EtOH are less negative than MeOH.

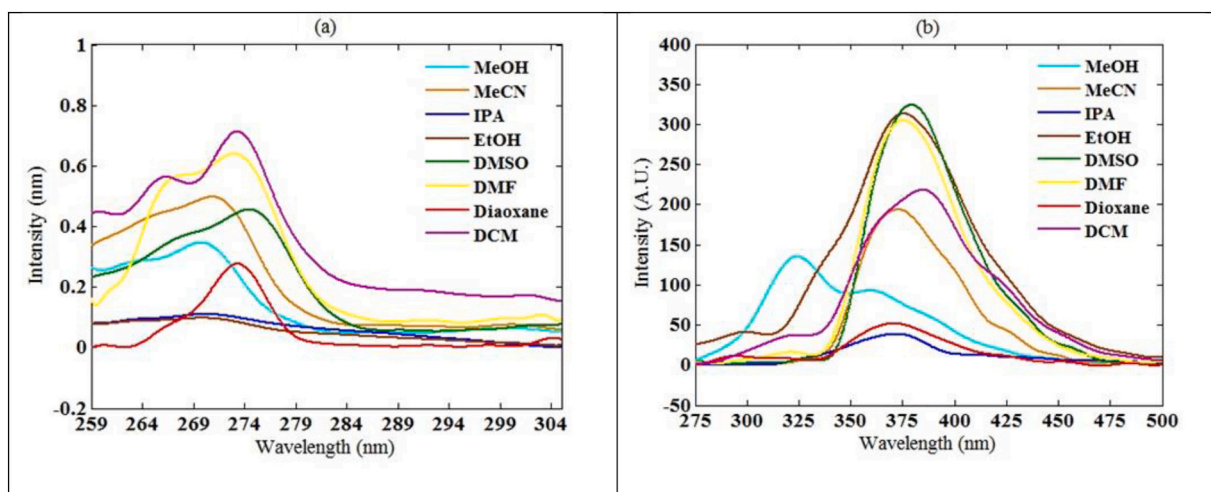
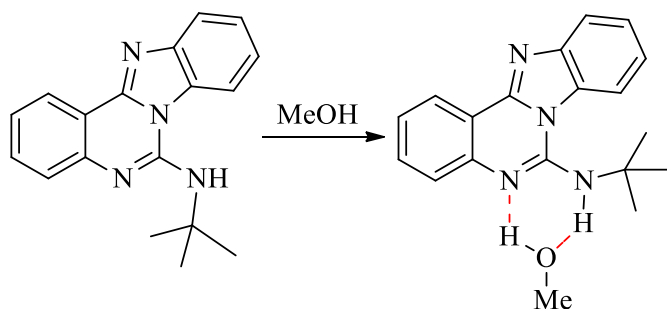


Fig. 1. UV – vis absorption spectrum (left) and fluorescence spectra (right) of **3a** (1×10^{-6} M) at room temperature excited at 272 nm.



Scheme 3. A schematic formation of a hydrogen bonded coordination pair.

This demonstrates that the creation of hydrogen-bonded complexes of **3a** with MeOH is more favorable (ESI). Moreover, the stabilizing effect of the solvent on the gas phase of the **3a** was examined. For this purpose, compound **3a** was optimized using B3LYP/6-31 + G(d,p) computational level in the gas phase and all tested solvents in this research. As can be seen in Table S3 (ESI), it is obvious that **3a** is more stabilized in all

solvents rather than the gas phase. It is notable that **3a** is more stable (-915.8677 Hartree) in methanol compared to other solvents.

Compared to the excited state, the hydrogen bond makes **3a** and its HOMO orbital more stable in the excited state. The total energy of gas phase, ground, and excited states of **3a** were calculated using B3LYP/6-31 + G(d,p) and PCM model for MeOH. As shown in Fig. S8 (ESI), methanol solvent makes **3a** and its HOMO more stabilized in the ground state than the excited state. In order to receive a more precise perspective of the fluorescent properties of **3a** in methanol, the F2-(MeOH)₂ hydrogen-bonded structure was selected, and the lowest 15 singlet-singlet transitions were calculated at B3LYP/Def2-TZVP computational level. The fluorescent properties such as transition Oscillatory strength (f), molecular orbitals transitions, and contributions of F2-(MeOH)₂ are represented in Table S4 (ESI). According to Table S4, the main molecular orbitals transition which creates λ_{max} in absorption and emission are HOMO-1 \rightarrow LUMO+1 (69.61%) and LUMO+1 \rightarrow HOMO-1 (62.91%), respectively. Fig. S9 (ESI) represents molecular orbital diagrams, energy level, and shape of LUMO+1 and HOMO-1 orbitals. The energy difference between LUMO+1 and HOMO-1 orbitals equals 5.014 eV.

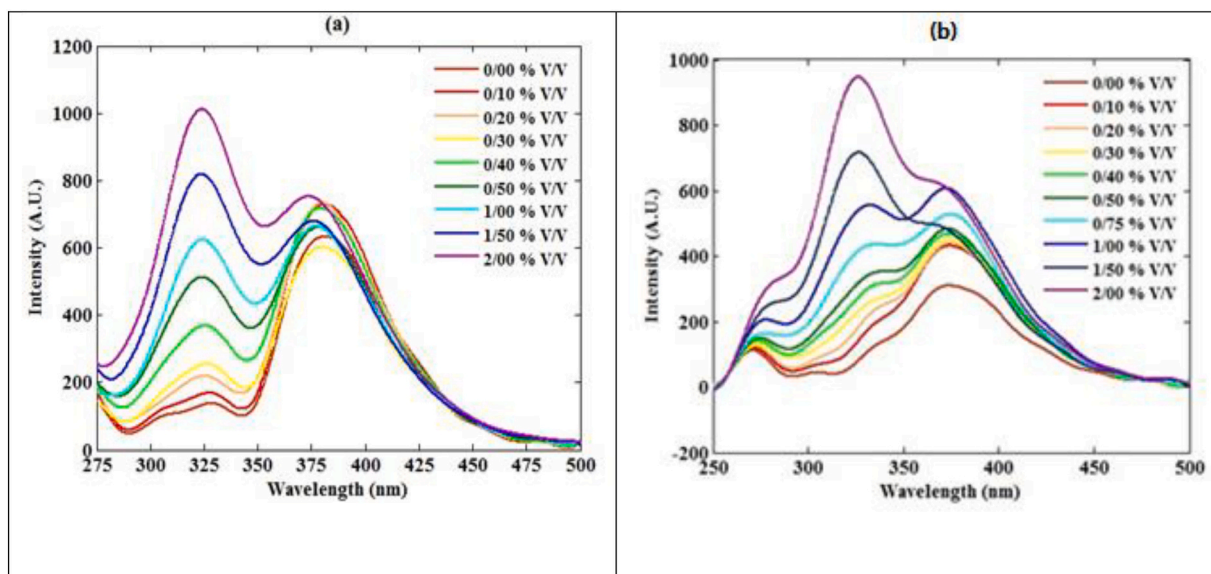
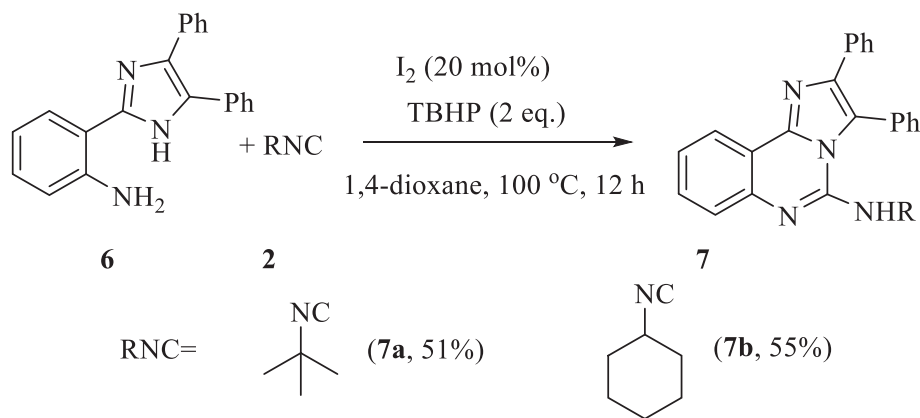


Fig. 2. Changes in emission of **3a** (1×10^{-6} M) in MeCN upon addition of MeOH. $\lambda_{ex} = 272$ nm (left) and changes in emission of **3a** (1×10^{-6} M) in EtOH upon addition of MeOH. $\lambda_{ex} = 272$ nm (right).



Scheme 4. Synthesis of 2,3-diphenylimidazo[1,2-c]quinazolin-5-amine

The above resulting data show the ability of the synthesized skeleton to detect the methanol by monitoring its emission spectra in the protic media. This particular solvatochromic behavior was tested for the MeOH levels detection in acetonitrile solvent. It was found that an increase in the level of MeOH led to an increase in fluorescence intensity (Fig. 2-left). A linear correlation was found between the amount of MeOH added and the fluorescence intensity (ESI). Although methanol and ethanol have the same properties, they have numerous effects on health and the environment. Consequently, in the pharmaceutical and chemical industries and forensic fields, MeOH-EtOH discrimination is significant [26]. The particular solvatochromic behavior for MeOH has therefore been investigated in EtOH solvent (Fig. 2-right). A low-intensity unstructured emission response was observed for **3a** in EtOH. An increment in MeOH (v/v%) was found to have resulted in a regular increase in intensity. A linear correlation was found between the amount of MeOH added and the intensity of fluorescence (ESI), with a limit of detection of 0.1529 V/V % and a quantification limit of 0.5099 V/V %. As a result, the **3a** demonstrated high sensitivity to MeOH detection in ethanol. It can be utilized for the quality control of alcoholic drinks by calculating the percentage of MeOH.

Finally, to further explore the isocyanide insertion strategy, we investigated the reaction of 2-(4,5-diphenyl-1H-imidazole-2-yl)aniline **6** and isocyanide **2** under optimized reaction conditions. The desired product N-(tert-butyl)-2,3-diphenylimidazo[1,2-c]quinazolin-5-amine **7** was obtained in good isolated yield (Scheme 4).

4. Conclusion

In conclusion, a metal-free and environmentally benign iodine-mediated isocyanide insertion reaction was developed for the benzimidazoquinazoline scaffold synthesis as new solvatochromic dyes. The transition metal-free and inexpensive catalysis, the ready availability of starting materials, broad substrate scope, high efficiency, and simple experimental procedure are advantages of this work. The emission spectrum of the synthesized skeleton was investigated in different polar solvents. Gratefully, it showed a selective blue shift in MeOH and can be utilized as an efficient and applicable probe for the selective MeOH monitoring.

CRedit authorship contribution statement

Fereshteh Ahmadi: Methodology, Data curation, Writing - original draft. **Nafiseh Ahmadi:** Methodology, Software. **Yaser Balmohammadi:** Formal analysis, Data curation. **Mohammad Reza Naimi-Jamal:** Supervision, Validation. **Ayoob Bazgir:** Supervision, Writing - review & editing.

Declaration of Competing Interest

The authors declare that they have no known competing financial interests or personal relationships that could have appeared to influence the work reported in this paper.

Acknowledgments

We gratefully acknowledge the financial support from the Research Council of Shahid Beheshti University and the Iran National Science Foundation (INSF) for the Post Doctoral Program (proposal number: 96011009).

Appendix A. Supplementary data

Supplementary data to this article can be found online at <https://doi.org/10.1016/j.catcom.2021.106331>.

References

- [1] M. Tian, Y. He, X. Zhang, X. Fan, Synthesis of Pyrazolo [5, 1-a] isoindoles and Pyrazolo [5, 1-a] isoindole-3-carboxamides through one-pot cascade reactions of 1-(2-Bromophenyl) buta-2, 3-dien-1-ones with isocyanide and hydrazine or acetohydrazide, *J. Organomet. Chem.* 80 (2015) 7447–7455.
- [2] J.W. Collet, T.R. Roose, E. Ruijter, B.U.W. Maes, R.V.A. Orru, Base metal catalyzed isocyanide insertions, *Angew. Chem. Int. Ed.* 59 (2020) 540–558.
- [3] A.H. Shinde, S. Arepally, M.D. Baravkar, D.S. Sharada, Nickel-catalyzed aerobic oxidative isocyanide insertion: access to benzimidazoquinazoline derivatives via a sequential double annulation cascade (SDAC) strategy, *J. Organomet. Chem.* 82 (2017) 331–342.
- [4] G. Qiu, Q. Ding, J. Wu, Recent advances in isocyanide insertion chemistry, *Chem. Soc. Rev.* 42 (2013) 5257–5269.
- [5] P. Bora, G. Bez, Chemoselective isocyanide insertion into the N–H bond using iodine–DMSO: metal-free access to substituted ureas, *Chem. Commun.* 54 (2018) 8363–8366.
- [6] F. Bandehali-Naeini, M. Shiri, B. Ramezani, S. Rajai-Daryasarei, Quinoline-based Polycyclic heterocycles by a hydrogen peroxide-mediated isocyanide insertion, *Polycycl. Aromat. Compd.* (2019) 1–9.
- [7] T.Q. Wei, P. Xu, S.Y. Wang, S.J. Ji, I₂/CHP-mediated oxidative coupling of 2-aminobenzamides and isocyanides: access to 2-aminoquinazolinones, *Eur. J. Org. Chem.* 32 (2016) 5393–5398.
- [8] H.X. Wang, T.Q. Wei, P. Xu, S.Y. Wang, S.J. Ji, I₂/TBHP-mediated oxidative coupling of amino-based bisnucleophiles and isocyanides: access to 2-aminobenzoxazinones, 2-aminobenzoxazines, and 2-aminoquinazolines under metal-free conditions, *J. Organomet. Chem.* 83 (2018) 13491–13497.
- [9] D. Liu, A. Lei, Iodine-catalyzed oxidative coupling reactions utilizing CH and XH as nucleophiles, *Chem. Asian J.* 10 (2015) 806–823.
- [10] W. Zhang, K. Xu, L. Yue, Z. Shao, Y. Feng, M. Fang, Two-dimensional carbazole-based derivatives as versatile chemosensors for colorimetric detection of cyanide and two-photon fluorescence imaging of viscosity in vitro, *Dyes Pigments* 137 (2017) 560–568.
- [11] X. Du, H. Hao, A. Qin, B.Z. Tang, Highly sensitive chemosensor for detection of methamphetamine by the combination of AIE luminogen and cucurbit [7] uril, *Dyes Pigments* 180 (2020) 108413–108435.
- [12] F. Miao, B. Tao, P.K. Chu, Nickel-palladium nanoparticles for nonenzymatic methanol detection, *Anal. Lett.* 45 (2012) 1447–1453.

- [13] U. Saha, M. Dolai, G.S. Kumar, Adaptable sensor for employing fluorometric detection of methanol molecules: theoretical aspects and DNA binding studies, *New J. Chem.* 43 (2019) 8982–8992.
- [14] M. Faisal, S.B. Khan, M.M. Rahman, A. Jamal, M.M. Abdullah, Fabrication of ZnO nanoparticles based sensitive methanol sensor and efficient photocatalyst, *Appl. Surf. Sci.* 258 (2012) 7515–7522.
- [15] W.I.S. Galpothdeniya, B.P. Regmi, K.S. McCarter, S.L. de Rooy, N. Siraj, I. M. Warner, Virtual colorimetric sensor array: single ionic liquid for solvent discrimination, *Anal. Chem.* 87 (2015) 4464–4471.
- [16] L. Yan, J. Liao, L. Feng, X. Zhao, L. Liang, W. Xing, C. Liu, Developing and performance measurements for a novel miniaturized electrochemical methanol sensor, *J. Electroanal. Chem.* 688 (2013) 49–52.
- [17] H. Ihmels, A. Meiswinkel, C.J. Mohrschlatt, Novel fluorescence probes based on 2, 6-donor–acceptor-substituted anthracene derivatives, *Org. Lett.* 2 (2000) 2865–2867.
- [18] S. Park, H.J. Kim, Highly activated Michael acceptor by an intramolecular hydrogen bond as a fluorescence turn-on probe for cyanide, *Chem. Commun.* 46 (2010) 9197–9199.
- [19] J. Wu, W. Liu, J. Ge, H. Zhang, P. Wang, New sensing mechanisms for design of fluorescent chemosensors emerging in recent years, *Chem. Soc. Rev.* 40 (2011) 3483–3495.
- [20] J. Shao, H. Sun, H. Guo, S. Ji, J. Zhao, W. Wu, X. Yuan, C. Zhang, T.D. James, A highly selective red-emitting FRET fluorescent molecular probe derived from BODIPY for the detection of cysteine and homocysteine: an experimental and theoretical study, *Chem. Sci.* 3 (2012) 1049–1061.
- [21] R.F. Landis, M. Yazdani, B. Creran, X. Yu, V. Nandwana, G. Cooke, V.M. Rotello, Solvatochromic probes for detecting hydrogen-bond-donating solvents, *Chem. Commun.* 50 (2014) 4579–4581.
- [22] S. Petrova, Y. Kostov, K. Jeffris, G. Rao, Optical ratiometric sensor for alcohol measurements, *Anal. Lett.* 40 (2007) 715–727.
- [23] T. Qin, B. Liu, Y. Huang, K. Yang, K. Zhu, Z. Luo, P. Chengjun, L. Wang, Ratiometric fluorescent monitoring of methanol in biodiesel by using an esipt-based flavonoid probe, *Sensors Actuators B Chem.* 277 (2018) 484–491.
- [24] J. Wang, M. Jiang, L. Yan, R. Peng, M. Huangfu, X. Guo, Y. Li, P. Wu, Multifunctional luminescent Eu (III)-based metal–organic framework for sensing methanol and detection and adsorption of Fe (III) ions in aqueous solution, *Inorg. Chem.* 55 (2016) 12660–12668.
- [25] Z. Wu, X. Fu, Y. Wang, Click synthesis of a triphenylamine-based fluorescent methanol probe with a unique D- π -A structure, *Sensors Actuators B Chem.* 245 (2017) 406–413.
- [26] S.S. Bag, S. Jana, Axially chiral amino acid scaffolds as efficient fluorescent discriminators of methanol–ethanol, *New J. Chem.* 41 (2017) 13391–13398.
- [27] C.K. Chang, C.W. Bastiaansen, D.J. Broer, H.L. Kuo, Discrimination of alcohol molecules using hydrogen-bridged cholesteric polymer networks, *Macromolecules* 45 (2012) 4550–4555.
- [28] S. Lv, S. Jie, B.-G. Li, Highly active and stereospecific polymerization of 1,3-butadiene catalyzed by bis{[2-(4,5-diphenylimidazolyl)phenylimino]phenolate}cobalt (II) complexes, *J. Organomet. Chem.* 799–800 (2015) 108–114.
- [29] P. Ghosh, A. Kumar Nandi, G. Chhetri, S. Das, Generation of ArS- and ArSe-substituted 4-quinolone derivatives using sodium iodide as an inducer, *J. Organomet. Chem.* 83 (2018) 12411–12419.
- [30] C. Tan, X. Liu, H. Jia, X. Zhao, J. Chen, Z. Wang, J. Tan, Practical synthesis of phosphinic amides/phosphoramidates through catalytic oxidative coupling of amines and P(O)–H compounds, *Chem. Eur. J.* 26 (2020) 881–887.
- [31] Z. Yang, J. He, Y. Wei, W. Li, P. Liu, KI/TBHP-promoted [3 + 2] cycloaddition of pyrrolo[1,2-a]quinoxalines and N-arylsulfonylhydrazones, *Org. Biomol. Chem.* 18 (2020) 3360–3366.
- [32] K. Krishnaveni, M. Iniya, D. Jeyanthi, A. Siva, D. Chellappa, A new multifunctional benzimidazole tagged coumarin as ratiometric fluorophore for the detection of Cd²⁺ and F[–] ions and imaging in live cells, *Spectrochim. Acta A: Mol. Biomol. Spect.* 205 (2018) 557–567.
- [33] M. Iniya, B. Vidya, T. Anand, G. Sivaraman, D. Jeyanthi, K. Krishnaveni, D. Chellappa, Microwave-assisted synthesis of imidazoquinazoline for chemosensing of Pb²⁺ and Fe³⁺ and living cell application, *Chem. Select* 3 (2018) 1282–1288.
- [34] M. Zakerhamidi, A. Ghanadzadeh, M. Moghadam, Solvent effects on the UV/visible absorption spectra of some aminoazobenzene dyes, *Chem. Sci. Trans.* 1 (2012) 1–8.
- [35] M.G. Mohamed, F.H. Lu, J.L. Hong, S.W. Kuo, Strong emission of 2, 4, 6-triphenylpyridine-functionalized polytyrosine and hydrogen-bonding interactions with poly (4-vinylpyridine), *Polym. Chem.* 6 (2015) 6340–6350.